Liquid Crystals
Publication details, including instructions for authors and subscription information:
http://www.informaworld.com/smpp/title~content=t713926090

Smectic liquid-crystalline phases of $F(CF_2)_7(CHOH)(CH_2)_8H$ and $F(CF_2)_9(CHOH)(CH_2)_{10}H$ Comparison with other partially fluorinated molecules

Patricia M. Vilalta[a]; Richard G. Weiss[a]
[a] Department of Chemistry, Georgetown University, Washington, D.C., U.S.A.

To cite this Article Vilalta, Patricia M. and Weiss, Richard G.(1992) 'Smectic liquid-crystalline phases of $F(CF_2)_7(CHOH)(CH_2)_8H$ and $F(CF_2)_9(CHOH)(CH_2)_{10}H$ Comparison with other partially fluorinated molecules', Liquid Crystals, 12: 4, 531 — 544

To link to this Article: DOI: 10.1080/02678299208029091

URL: http://dx.doi.org/10.1080/02678299208029091

Liquid Crystals, 1992, Vol. 12, No. 4, 531–544

Smectic liquid-crystalline phases of $F(CF_2)_7(CHOH)(CH_2)_8H$ and $F(CF_2)_9(CHOH)(CH_2)_{10}H$ Comparison with other partially fluorinated molecules

by PATRICIA M. VILALTA and RICHARD G. WEISS*
Department of Chemistry, Georgetown University,
Washington, D.C. 20057, U.S.A.

(*Received 28 January 1992; accepted 28 April 1992*)

Partially fluorinated alcohols $F(CF_2)_m(CHOH)(CH_2)_nH$ (where $m = 7$, $n = 8$ and $m = 9$, $n = 10$) exhibit highly ordered smectic liquid-crystalline phases, as confirmed by optical microscopy and differential scanning calorimetry. Miscibility studies show that the smectic phases of the two alcohols are not of the same type. The related partially fluorinated ketones $F(CF_2)_mCO(CH_2)_nH$ do not form a detectable mesophase. This is rather surprising since the (more polar) corresponding alcohols and the (less polar) analogous iodides and *n*-alkanes do. A brief discussion of the results and a comparison among partially fluorinated alkanes with various functional groups are presented.

1. Introduction

Recently, investigations of the properties of compounds consisting of fluorocarbon and hydrocarbon segments (i.e. diblock molecules) have received a great deal of attention [1–11]. Partially fluorinated *n*-alkanes F*m*H*n* have been the most extensively studied [1–8, 11]. Among other properties, they are primitive (non-ionic and non-polar) surfactants which can form normal and reversed micelles [1]. When mixed with simple hydrocarbon solvents, an organized gel-like structure can be formed [2, 3].

In some homologues of F*m*H*n*, more than one solid [4, 5] or smectic liquid-crystalline phase [6–8] has been detected. For instance, perfluorodecyl decane (F10H10) forms two smectic G or J phases in which the extended molecules are packed in layers in a pseudo-hexagonal fashion and are tilted relative to the layer normal [6, 8].

Fluorocarbon–hydrocarbon diblock molecules with an allyl ether [10, 11] and a methacrylate [11] group at the end of the chain (F*m*H*n*O–CH2–CH=CH2 and F*m*H*n*O2C(CH3)C=CH2, respectively) exhibit either one or two smectic transitions before melting; some ω-perfluoroalkyl-1-alkanols F*m*H*n*OH also show smectic phases [10, 11].

Given these observations, we anticipated that partially fluorinated alkanes, substituents near the middle of a carbon chain, might also be mesomorphic. In fact, Viney *et al.* [9] have reported that iodo-substituted partially fluorinated alkanes (F10(CH2CHI)H*n*, $4 \leqslant n \leqslant 10$) form enantiotropic smectic B liquid-crystalline phases over a relatively broad temperature range and smectic A phases over a much narrower range. Secondary alcohols (F*m*(CHOH)H*n*) [12, 13] and ketones (F*m*COH*n*) [14, 15] which are somewhat shorter than the mesomorphic iodides have been synthesized but

---

* Author for correspondence.

there is no mention of their possible liquid-crystalline behaviour. We have synthesized two alcohols (F7(CHOH)H8 and F9(CHOH)H10) and ketones (F7COH8 and F9COH10) of lengths comparable to those of the mesomorphic iodides and find, surprisingly, that the alcohols are liquid-crystalline [16]. In each case, the attribution of phase type is based upon a combination of thermograms from differential scanning calorimetry and birefringent patterns from optical microscopy.

$F(CF_2)_m(CH_2)_nH$
F*m*H*n*

$F(CF_2)_mCO(CH_2)_nH$
F*m*COH*n*

$F(CF_2)_m(CH_2\text{–}CHI)(CH_2)_nH$
F*m*(CH2CHI)H*n*

$F(CF_2)_m(CH_2)_nOH$
F*m*H*n*OH

$F(CF_2)_m(CHOH)(CH_2)_nH$
F*m*(CHOH)H*n*

2. Experimental

1-Bromooctane (Aldrich, 99 per cent), 1-bromodecane (Aldrich, >98 per cent), perfluorooctanoic acid (PCR, 99 per cent *n*-isomer) and perfluorodecanoic acid (PCR, 97 per cent *n*-isomer) were used as received. Anhydrous diethyl ether (Fisher) was refluxed and distilled from $LiAlH_4$ prior to use.

Heats of transition and temperatures of maximum heat flow were measured with a Dupont 1090B thermal analyser and a 910 DSC cell base. Samples (*c*. 3–6 mg) were sealed in two-piece aluminium pans. Temperatures were calibrated with an indium standard and then referenced daily to the Phase I→Phase II and Phase II→isotropic transition temperatures of heneicosane.

For neat partially fluorinated alcohol samples, thermograms were recorded while material was heated to *c*. 10° above its optically detected clearing temperature (scan 1), cooled to *c*. 25°C (scan 2), and heated immediately as in scan 1 (scan 3). Thermograms of binary mixtures were recorded after samples had been heated to *c*. 10° above their clearing temperature and maintained there for at least 40 min, since samples were directly weighed into the aluminium pans. Unless otherwise noted, reported data are an average from at least two determinations and heating and cooling rates were $2° \min^{-1}$. Due to hysteresis, heat of transition for S_2–S_1 is of limited use. Transition temperatures (corrected) were measured optically on a Bausch and Lomb microscope (×100) equipped with a Kofler hot stage and crossed polars above and below the sample. Photographs were taken with a Nikon Optiphot microscope equipped with a hot stage, crossed polars, and a Nikon FX-35 WA camera (total magnification: ×688). NMR spectra were obtained with a Bruker AM-300 WM spectrometer using an Aspect 3000 computer and a Bruker 5 mm probe (^1H, ^{13}C, and ^{19}F). We have previously reported the ^{19}F chemical shifts as negative with respect to $CFCl_3$, according to Harris [17]; here they are reported as positive according to the convention used by Dungan [18]. IR spectra were recorded on either a Perkin–Elmer 457 grating spectrophotometer (polystyrene reference) or a Mattson Instruments 2020 Galaxy Series FT-IR spectrophotometer. Either a NaCl cell was used for solution experiments or AgCl plates for neat samples. Temperature experiments were carried out in a thermostatted cell holder designed for use with samples of this sort. Purity was determined by analytical gas chromatography (GLPC) using a Hewlett Packard 5890A, gas chromatograph equipped with flame ionization (FID) and thermal conductivity detectors (TCD) and a wide bore fused silica open tubular capillary CP-Sil-19 CB column (0·53 mm × 10 m). Peaks were quantified using a Hewlett Packard 3393A integrator. Elemental analyses were determined by Desert Analytics, Tucson, Arizona.

2.1. *Synthesis of diblock compounds*

Partially fluorinated alcohols F*m*(CHOH)H*n* were synthesized by reduction with $LiAlH_4$ of the respective ketones F*m*COH*n* which were prepared by a modification of a method outlined by Dishart and Levine [14].

2.1.1. *Synthesis of F9COH10*

Under a dry nitrogen atmosphere, at ambient temperature, one third of a solution of 5·1 g (0·023 mol) of 1-bromodecane in 8 ml of dry diethyl ether was added dropwise to 0·8 g (0·03 g-atom) of magnesium ribbon in 6 ml of dry diethyl ether. After reaction had initiated, 12 ml of dry diethyl ether and the remaining 1-bromodecane solution were added dropwise and the reaction mixture was refluxed for 1 h. It was cooled to room temperature, and 4·0 g (7·8 mmol) of perfluorodecanoic acid in 35 ml of dry diethyl ether was added dropwise. After being refluxed for 4 h, the reaction vessel was cooled in a crushed ice bath and then quenched with *c.* 2 : 2 : 6 (w : v : v) $NH_4Cl : HCl : H_2O$ buffer solution until pH 2–3 was reached. The mixture was extracted several times with diethyl ether. The combined organic layers were washed with sodium bicarbonate, dried with anhydrous magnesium sulphate, filtered, and evaporated to residue on a rotatory evaporator. The residue was purified by passage through a silica gel column (Baker Analyzed, 60–200 mesh) using hexane as eluent. The yield of ketone ($\geqslant$99 per cent pure by GLPC after recrystallization from ethanol or acetonitrile) was 20–25 per cent in our best runs. The coupling product, eicosane, and several unidentified compounds were produced also. No attempts were made to optimize yields.

F9COH10: mp 42·2–43·0°C. IR (film): 3000–2800 (C–H stretching), 1770–1740 ((carbonyl vibration), 1470–1440 (weak, CH_2 bend), 1300–1100 cm^{-1} (C–F vibration). ^1H NMR ($CDCl_3$, TMS): δ 0·9 (t, 2·6 H, $-CH_3$), 1·3 (br s, 13·7 H, $-(CH_2)_7-$), 1·7 (m, 2·1 H, $-C\underline{H}_2-CH_2-CO-$), 2·7 ppm (t, 2·3 H, $-C\underline{H}_2-CO-$). ^{13}C NMR ($CDCl_3$): δ 194·2 (t, $J \approx 25$ Hz, carbonyl), 38·0, 32·0, 29·6, 29·5, 29·3, 28·8, 22·8, 22·5, and 14·1 ppm; carbon atoms attached to fluorine were weakly detected as multiplets near 105–124 ppm. ^{19}F NMR ($CDCl_3$, $CFCl_3$): δ 81·2, (s, 3 F, $-CF_3$), 120·8, 121·8, 122·3, 122·7, 123·1 and 126·6 ppm (s, 16 F, $-(CF_2)_8-$). Elemental analysis: calculated for $C_{20}H_{21}OF_{19}$, C, 37·62 per cent; H, 3·29 per cent; F, 56·58 per cent, found, C, 37·66 per cent; H, 3·16 per cent; F, 56·72 per cent.

2.1.2. *Synthesis of F9(CHOH)H10*

Under a dry nitrogen atmosphere, 200 mg (0·31 mmol) of F9COH10 (in 4 ml of dry diethyl ether) was added dropwise to a stirred mixture of 20 mg (0·53 mmol) $LiAlH_4$ in 4 ml of dry diethyl ether. After being refluxed for 1–2 h, the reaction flask was cooled in a crushed ice bath and carefully quenched with a 2 : 2 : 6 (w : v : v) $NH_4Cl : HCl : H_2O$ buffer solution until pH 2–3 was reached. The mixture was extracted several times with diethyl ether and the combined organic layers were washed with sodium bicarbonate, dried over anhydrous magnesium sulphate, filtered, and reduced to residue on a rotatory evaporator. The residue was passed through a silica gel column (Baker Analyzed, 60–200 mesh). The eluent was changed from neat hexane initially to 50 : 50 hexane : methylene chloride. The partially fluorinated alcohol was obtained in 65–70 per cent yield ($\geqslant$99 per cent pure by GLPC) after recrystallization from acetonitrile.

F9(CHOH)H10: mp 86·2–87·2°C. IR (neat film): 3550–3200 (O–H vibration), 3000–2850 (C–H stretching), 1480–1430 (CH_2 bending), 1300–1100 (C–F and C–O vibrations). ^1H NMR ($CDCl_3$): δ 0·9 (t, 2·4 H, $-CH_3$), 1·3 (br s, methylenes, integrating for 15·1 H), 1·5–1·8 (multiplets, methylenes integrating for 3·1 H), 4·1 ppm (m, 1·2 H, $>C\underline{H}OH$), $O\underline{H}$ was detected as a doublet, overlapping with multiplets at 1·8 ppm; the doublet disappeared upon addition of one drop of D_2O. ^{13}C NMR ($CDCl_3$): δ 70·5 (t, $J \approx 25$ Hz, $-CF_2-\underline{C}HOH-$), 32·0, 29·6, 29·5, 29·4, 29·3, 25·1, 22·7 and 14·2 ppm. Carbons attached to fluorine were weakly detected as multiplets near 105–124 ppm. ^{19}F ($CDCl_3$, $CFCl_3$): δ 81·3 (3 F, CF_3), signals at 121·0, 122·0, 122·3, 123·2, 126·6, 127·6 integrating for 15·4 F ($-(CF_2)_8-$). Elemental analysis: calculated for $C_{20}H_{23}OF_{19}$, C, 37·50 per cent; H, 3·59 per cent; F, 56·41 per cent; found, C, 37·20 per cent; H, 3·58 per cent; F, 54·13 per cent.

F7COH8 and F7(CHOH)H8 were synthesized by similar procedures. Their spectroscopic properties and physical constants have been reported elsewhere [19].

3. Results and discussion

3.1. *Identification of phases*

Typical heating and cooling thermograms of the F*m*(CHOH)H*n* are shown in figures 1 and 2. For each alcohol, scans 2 and 3 can be reproduced by subsequent cooling and heating cycles. No additional transitions were detected in the samples upon cooling to or heating from −40°C. Phase diagrams which summarize the observations are included in the scheme. Broken lines indicate cooling and full lines indicate heating data. Slow transitions occurring at a constant temperature are indicated with an asterisk. The transitions are reported at temperatures of maximum heat flow. The total heats associated with the cooling exotherms (scan 2) are distinctly less than the heat absorbed during scan 3. Since the differences between the total heats are reproducible, cooling at $2°\,min^{-1}$ results in phases which are not totally at equilibrium (hysteresis) and which reorganize somewhat with time. The alcohols, as obtained from solvent recrystallization, are white and opaque, melting at 66·7–67·7°C (F7(CHOH)H8) and 86·2–87·2°C (F9(CHOH)H10) to transparent, non-birefringent fluids. We conjecture that the solvent-crystallized F7(CHOH)H8 is a solid while S_2 is a monotropic mesophase (*vide infra*). The S_1 phase of F7(CHOH)H8 has a distinct smectic birefringent pattern (see figure 3(*a*)). The heat associated with the F7(CHOH)H8 S_1–I transition is comparable to that observed for the S–I transition of perfluorodecyl decane ($-41·7\,J\,g^{-1}$) [6]. If S_1 is cooled only to 56°C and then reheated, the magnitude of its endotherm is about $2\,J\,g^{-1}$ larger than that of the S_1–I exotherm. Based upon the small S_1–S_2 heat of transition and the similarity of the S_1 and S_2 optical micrographs (compare figures 3(*a*) and (*b*)), we ascribe S_2 to a higher order smectic phase; the small spots in figure 3(*b*) are due to separation of the alcohol from the top cover slip as it contracts when cooled.

The transformation of S_2 to the thermodynamically more stable solid phase can be observed in annealed samples by optical microscopy and by differential scanning calorimetry. After a few hours at room temperature, a sample of initially S_2 F7(CHOH)H8 displays two heating endotherms at 61·6°C and 63·5°C. The heat of each transition is dependent upon the time which the S_2 phase is allowed to anneal. The total heat of the two transitions is greater than the S_2–I endotherm and increases with the relative importance of the transition centred at 63·5°C (see figure 4(*a*)).

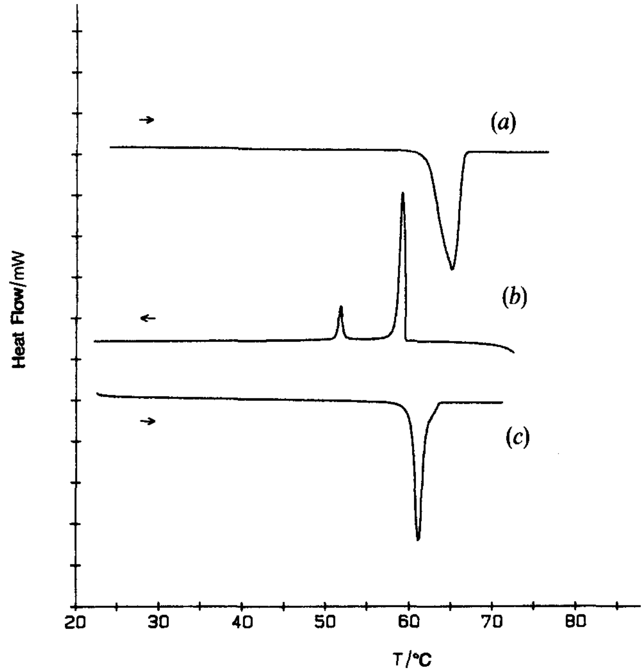

Figure 1. F7(CHOH)H8 thermograms, scanned at 2° min^{-1}. Arrows indicate the direction of temperature change. (*a*) Solvent precipitated material (scan 1); (*b*) scan 2; (*c*) scan 3. The increments are 1 mW between marks on the ordinate.

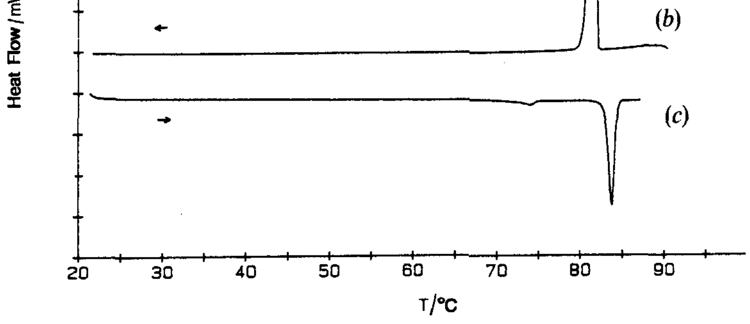

Figure 2. F9(CHOH)H10 thermograms, scanned at 2° min^{-1}. Arrows indicate the direction of temperature change. (*a*) Solvent precipitated material (scan 1); (*b*) scan 2; (*c*) scan 3. The increments are 2 mW between marks on the ordinate.

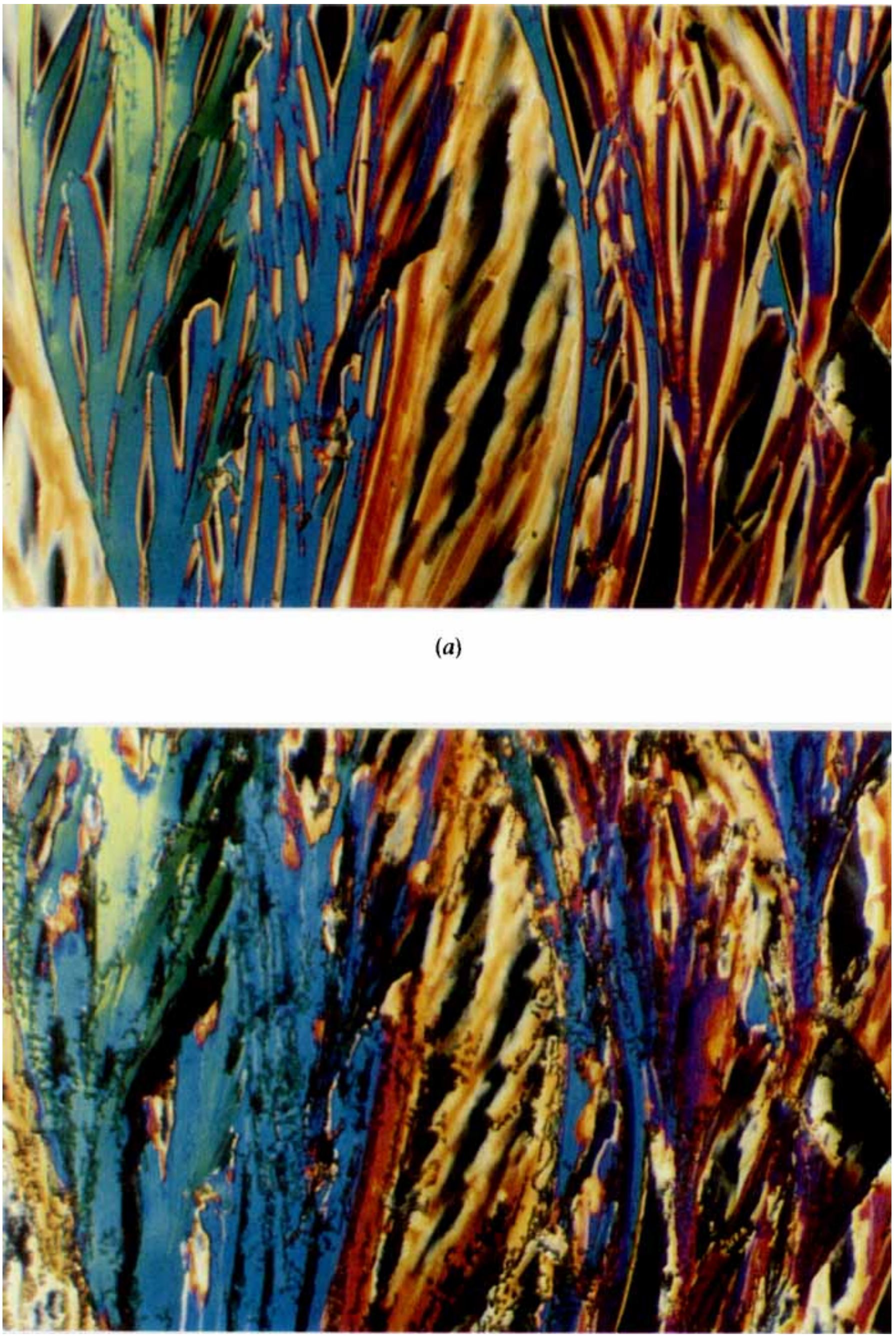

(*a*)

(*b*)

Figure 3. Optical micrographs showing the texture of F7(CHOH)H8 (magnification × 688). (*a*) S_1 (60·1°C); (*b*) S_2 (37·7°C).

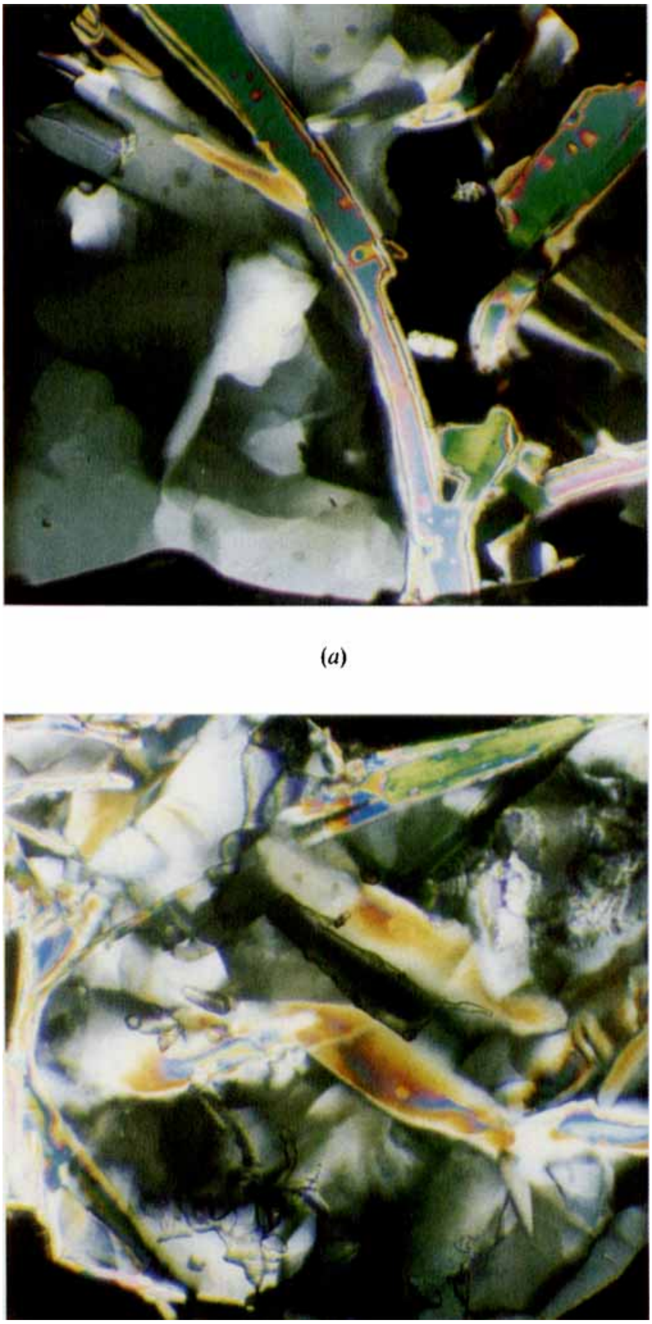

(*a*)

(*b*)

Figure 5. Optical micrographs showing the texture of F9(CHOH)H10 (magnification × 688). (*a*) S_1 (79°C, cooled from the isotropic phase); (*b*) S_2 (40°C).

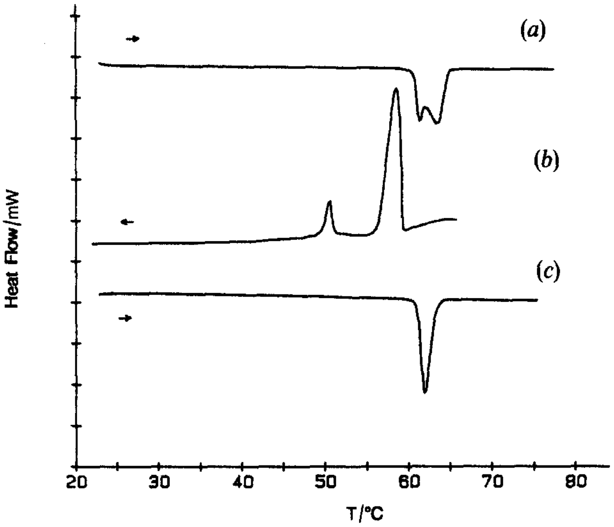

Figure 4. Thermograms of F7(CHOH)H8. (*a*) Sample annealed at room temperature; (*b*) scan 2; (*c*) scan 3. The increments are 2 mW between marks on the ordinate.

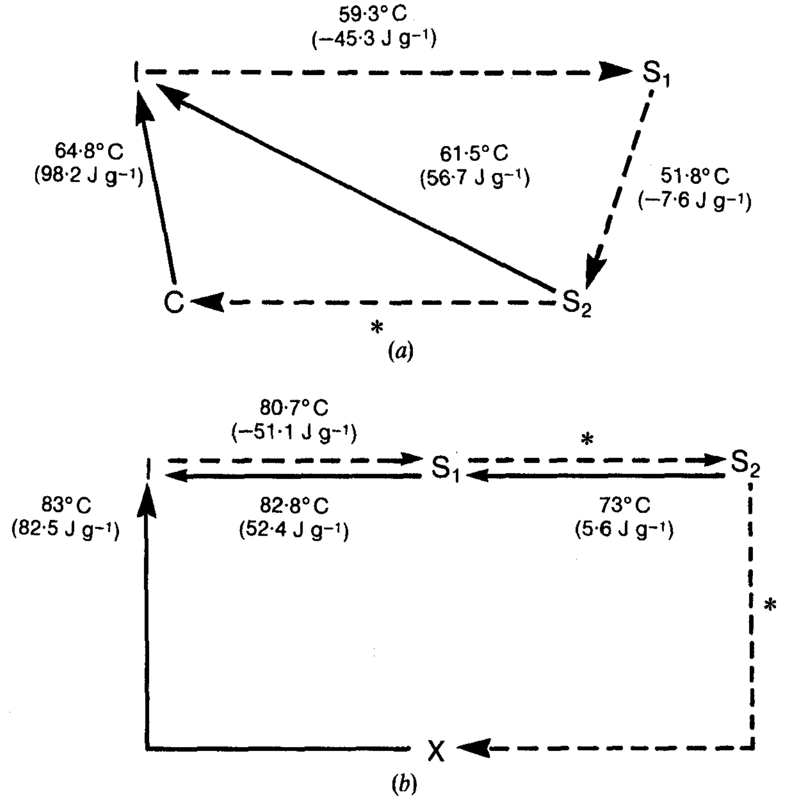

Phase transition temperatures and heats of transition for (*a*) F7(CHOH)H8 and (*b*) F9(CHOH)H10. Broken lines indicate cooling and full lines indicate heating data. Slow transitions occurring at a constant temperature are indicated with an asterisk.

It is not clear whether X, the F9(CHOH)H10 phase obtained upon precipitation from acetonitrile, is crystalline or liquid-crystalline. As indicated in the scheme and figure 2(*a*), it yields isotropic liquid directly when heated to 83°C. The optical micrograph taken immediately after cooling F9(CHOH)H10 below 80°C is characteristic of a smectic liquid crystal (see figure 5(*a*)). No additional exotherms were detectable upon further cooling to room temperature (see figure 2(*b*)). However, subsequent heating thermograms contain two endotherms corresponding to S_1–S_2 at 73°C and S_1–I at 82·8°C (see figure 2(*c*)). Although the transition temperatures to the isotropic phase from the first and second heating scans are the same, the sum of the enthalpies of the endotherms from the second heating are less than the enthalpy of the single transition from the first heating. The small heat associated with the S_1–S_2 transition and our inability to differentiate it from S_1 by optical microscopy lead us to believe that there is little reorganization of molecules between S_2 and S_1 and that S_2 is probably smectic, also. Thus, the X phase obtained from solvent recrystallization must be either a crystal or a higher order smectic.

The lack of a second detectable exotherm during the cooling of F9(CHOH)H10 indicates that formation of the S_2 phase is a slow process. Thus, no transition at 73°C can be detected upon heating a sample which had been cooled from the isotropic to 65°C and left there for 30 min; the same protocol, but with incubation at 60°C, results in an endotherm at 73°C. In fact, both the heat and temperature of the S_1–S_2 transition are very dependent on the heating and cooling rates of the DSC scans. As mentioned, rates of 2° min^{-1} were employed to construct the scheme (*b*).

After annealing a sample of F9(CHOH)H10 at room temperature for several weeks, its heating thermogram showed that it had reverted partially to phase X (see figure

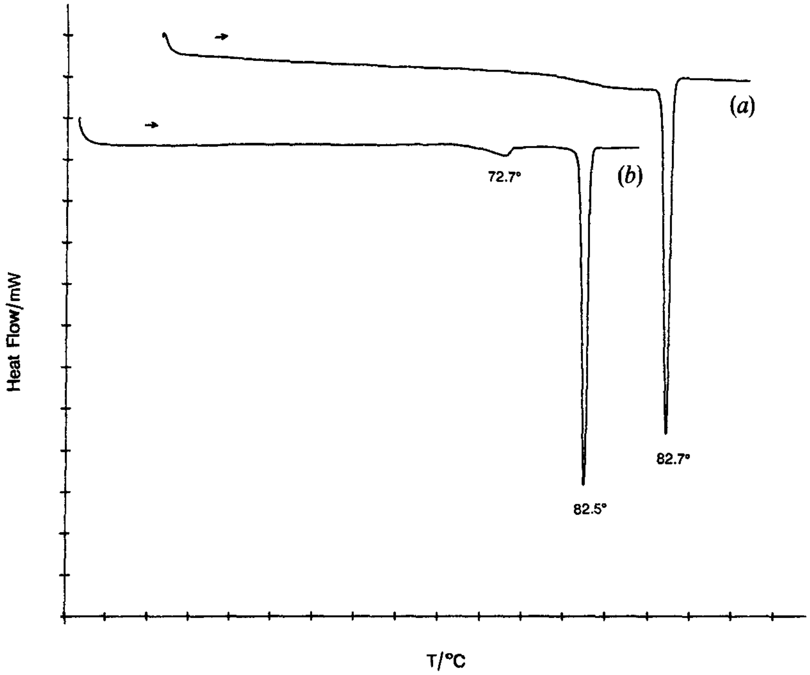

Figure 6. Thermograms of F9(CHOH)H10. (*a*) Sample annealed at room temperature for a few weeks; (*b*) reheated immediately after (*a*). The increments are 0·5 mW between marks on the ordinate and 5° between marks on the abscissa.

6 (*a*)). We attribute the broad, lower temperature endotherm to S_2 transforming to S_1 in the presence of some X. The total endothermicity of the heating scan (72·2 J g^{-1}) is intermediate between that found from pure X (82·5 J g^{-1}) and from previously melted material (58 J g^{-1}).

The birefringent optical patterns associated with the S_1 and S_2 phases of F9(CHOH)H10 are shown in figure 5. They differ markedly from the optical patterns of F7(CHOH)H8 (see figure 3); in fact, the phases of the two homologues are clearly different. A cooling–heating thermogram of a binary mixture of 47/53 (w/w) F7(CHOH)H8/F9(CHOH)H10 shows broad transitions between 40°C and 70°C (see figure 7), indicating a slow and gradual melting of the alcohols. Samples of the two homologues, placed in edge contact on a glass plate and observed under a microscope, did not coalesce to one phase upon being heated or cooled. On these bases, we conclude that F7(CHOH)H8 and F9(CHOH)H10 form different types of smectic phases at common temperatures [20].

3.2. *IR studies*

IR spectra of neat F7(CHOH)H8 and F9(CHOH)H10 samples at room temperature show a strong, broad band at ~3400 cm^{-1} due to O–H--F and/or O–H--O hydrogen bonding [21]. The infrared spectra of the alcohols in CCl_4 (*c*. 3×10^{-2} M) display sharper O–H absorption peaks which are shifted to higher frequencies (*c*. 3600 cm^{-1}), and which may be attributed to vibrations of unassociated O–H groups [21]. In its isotropic phase at 67°C, neat F7(CHOH)H8 displays an OH stretching band centred near 3450 cm^{-1} which is more intense and somewhat sharper than in its smectic phase at room temperature. Upon sample cooling, the band becomes progressively broader and of slightly lower frequency. There are no abrupt changes in any of the IR spectral bands throughout the temperature range spanning the isotropic, S_1, and S_2 phases. Clearly, the hydrogen bonding interactions are largely intermolecular in the neat phases. Whatever packing arrangements occur within the smectic phases, they include strong intermolecular interactions (probably among hydroxy groups of neighbouring molecules).

3.3. *Comparison with other partially fluorinated compounds*

DSC experiments and microscopic analyses do not provide evidence for the presence of mesophases of the analogous ketones, F7COH8 and F9COH10. For

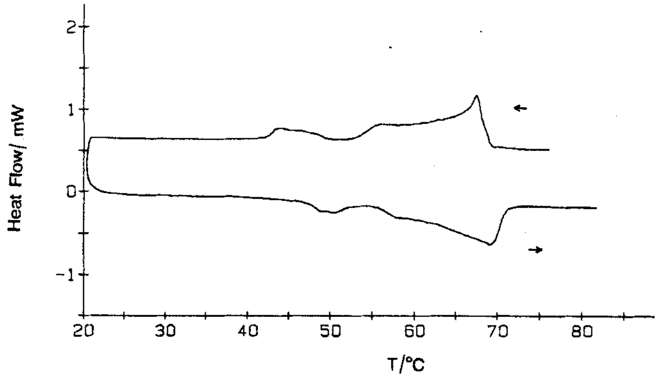

Figure 7. Thermogram of a 47/53 (*w*/*w*) F7(CHOH)H8/F9(CHOH)H10 mixture.

instance, we could not match the optical micrograph of F9COH10 (see figure 8) with that of a known nematic or smectic phase pattern in the books by Demus and Richter [22] and Gray and Goodby [23]. This is rather surprising since the more polar, partially fluorinated alcohols and the less polar, partially fluorinated iodides and *n*-alkanes do form mesophases (see the table). The cooling and heating thermograms of the ketones, reproducible between the first and subsequent scans, appear in figure 9.

The total enthalpy associated with the heating endotherms of the partially fluorinated ketones is higher than that of their alcohol counterparts (see the table), in spite of the fact that stronger intermolecular forces are possible between alcohols (if there are extensive hydrogen bonding interactions) than between ketones (if there are weakened dipole–dipole interactions of carbonyl groups). This apparent anomaly is explicable if the ketones are crystalline and the alcohols are liquid-crystalline in their highest temperature non-isotropic phase.

In this regard, it is instructive to compare the total heats of melting (for all transitions separating the lower temperature phases and isotropic liquids) and the clearing temperatures for the partially fluorinated molecules included in the table. The 'unsubstituted' partially fluorinated alkane, F10H10, exhibits highly ordered smectic phases [6, 7] whose heat of melting is *c.* 20 J g^{-1} higher than that of the analogous iodide, F10(CH2CHI)H8 [9]. One can imagine that a large iodine atom, located near the middle of a smectic layer, creates a net disruptive influence since its contribution to stabilizing intermolecular interactions through dipolar and dispersive forces is small; the van der Waals volume calculated for a CHI group is 24·62 cm^3 mol^{-1} [24, 25] and the group dipole of a C_{sp^3}–I bond is ~1·29 D [26]. The more polar ketone F9COH10 replaces two fluorine atoms of F10H10 with an oxygen atom of somewhat smaller van der Waals volume (calculated van der Waals volumes for C=O, CF_2, and CH_2 groups are 11·75, 16·04, and 10·22 cm^3 mol^{-1}, respectively [24, 25]). Thus, conceptually, the

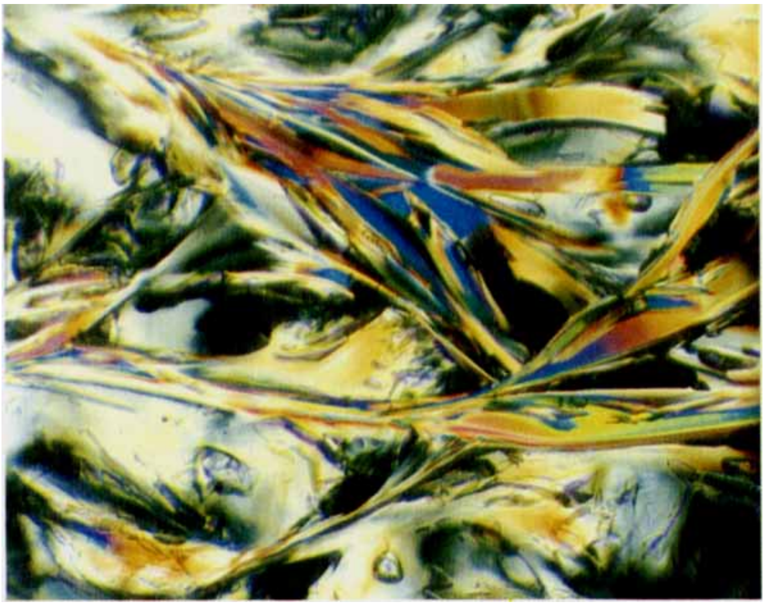

Figure 8. Optical micrograph showing the texture of F9COH10 (magnification × 688) at 37°C (cooled from the isotropic phase).

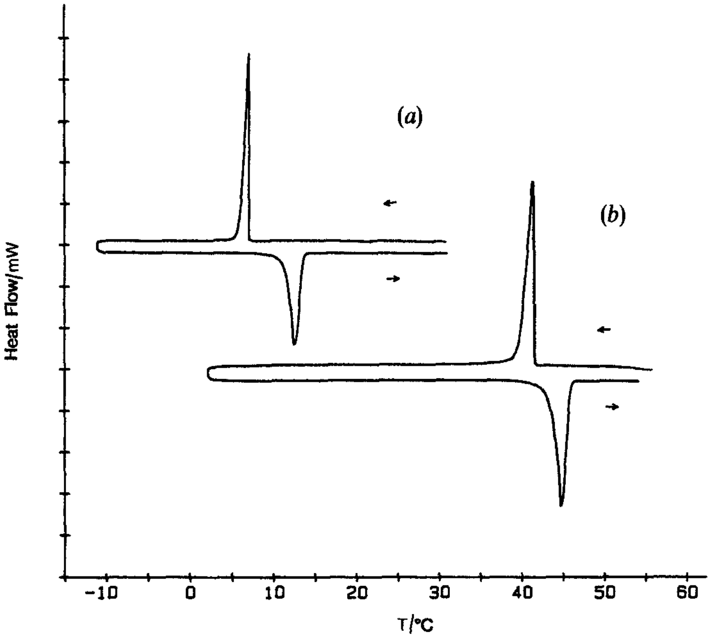

Figure 9. Thermograms of semifluorinated ketones, scanned at 2° min^{-1}. Direction of temperature change while scanning is indicated by arrows. (*a*) F7COH8; (*b*) F9COH10. The increments are 2 mW between marks on the ordinate.

ketone can pack like F10H10 but also may suffer weakened intermolecular dipolar interactions (which attenuate further translational motions) between carbonyl groups on neighbouring molecules: the group dipole for the carbonyl group of a dialkyl ketone is 2·4 D [26]; a perfluoroalkyl group should decrease that value due to its electron-withdrawing influence. The dipole–dipole interactions between neighbouring F*m*COH*n* molecules may also cause their packing arrangement to be very different from those of the related molecules which form smectic phases.

As judged from a comparison between the heats of melting of F9(CHOH)H10 (which places the hydroxyl group near the middle of the molecular chain) and F10H10OH (which also forms a smectic phase [11] and has its hydroxyl group at the end of the chain), it would appear that the location of the hydrogen bonding interactions within partially fluorinated alcohols is not very important; both molecules have high clearing temperatures and almost the same heats of melting. The similarity between these heats of melting may be fortuitous. The van der Waals volume calculated for a CHOH moiety (15·32 $\text{cm}^3\,\text{mol}^{-1}$ [24, 25]), being somewhat larger than that of a carbonyl group, may create a greater disturbance to packing near the middle of a layered assembly of molecules than its hydrogen bonding energy can overcome. At a molecular end (and layer boundary), the hydroxyl group may undergo intra and interlayer hydrogen bonding interactions without disturbing significantly other aspects of layer packing.

Clearly, the ideas set forth to explain the comparative values included in the table will require much more experimentation before they can be accepted or rejected. Specifically, X-ray analyses of many of these molecules (including the alcohols and ketones synthesized by us) in their various phases are lacking. Regardless, the interplay

Heats of transition and temperatures of partially fluorinated compounds.

	Mesophase formed	T_1/°C	ΔH_1/kJ mol^{-1}	T_i/°C	ΔH_i/kJ mol^{-1}	Heat of melting	
						$\Sigma\Delta H$/kJ mol^{-1}	$\Sigma\Delta H$/J g^{-1}
F7(CHOH)H8†	yes	(51·8)	(−3·9)	(59·3)	(−23·2)	(−27·1)	(−52·9)
F7COH8	no	—	—	12·6	34·2	34·2	67·0
F8H8 [11]	yes	28	9·5	30	5·7	15·2	28·6
F9(CHOH)H10	yes	73	3·6	82·8	33·5	37·1	58·0
F9COH10	no	—	—	44·7	53·1	53·1	83·3
F10H10OH [11]	yes	−8	3·4	103	35·1	38·5	57·0
F10(CH2CHI)H8 [9]	yes	—	—	54·8‡	19·2	19·2	24·4
F10H10 [6]	yes	37·3	2·2	63·5	26·7	28·9	43·8

† Values obtained from cooling scan.

‡ Onset temperature.

T_i = solid or smectic phase–isotropic transition (clearing temperatures).

T_1 = lower phase transition temperature.

of factors responsible for these partially fluorinated alkanes and centrally substituted iodides and alcohols being mesomorphic while the ketones are not is an intriguing observation which merits further study.

We are grateful to the National Science Foundation for its support of this research. We thank the Biomolecular Engineering Branch of the Naval Research Laboratory for the use of its optical microscope in obtaining the micrographs used in the manuscript and Dr Jens Höpken for sharing unpublished information concerning his terminally substituted partially fluorinated alcohols with us.

References

[1] Turberg, M. P., and Brady, J. E., 1988, *J. Am. chem. Soc.*, **110,** 7797.
[2] Pugh, C., Hopken, J., and Moller, M., 1988, *Polymer Preprints*, **29,** 460.
[3] Rabolt, J. F., Russell, T. P., Siemens, R., Twieg, R. J., and Farmer, B., 1986, *Polymer Preprints*, **27,** 223.
[4] Russell, T. P., Rabolt, J. P., Twieg, R. J., Siemens, R. L., and Farmer, B. L., 1986, *Macromolecules*, **19,** 1135.
[5] Rabolt, J. F., Russell, T. P., and Twieg, R. J., 1984, *Macromolecules*, **17,** 2786.
[6] Viney, C., Russell, T. P., Depero, L. E., and Twieg, R. J., 1989, *Molec. Crystals liq. Crystals*, **168,** 63.
[7] Mahler, W., Guillon, D., and Skoulios, A., 1985, *Molec. Crystals liq. Crystals Lett.*, **2,** 111.
[8] Viney, C., Twieg, R. J., Russell, T. P., and Depero, L. E., 1989, *Liq. Crystals*, **5,** 1783.
[9] Viney, C., Twieg, R. J., and Russell, T. P., 1990, *Molec. Crystals liq. Crystals*, **182B,** 291.
[10] Hopken, J., Moller, M., and Boileau, S., 1990, *Polymer Preprints*, **31,** 324.
[11] Hopken, J., 1991, Ph.D. Thesis, University of Twente, CIP-DATA Koninklijke Bibliotheek.
[12] Kitazume, T., and Ishikawa, N., 1985, *J. Am. chem. Soc.*, **107,** 5186.
[13] Kitazume, T., and Ikeya, T., 1988, *J. org. Chem.*, **53,** 2349.
[14] Dishart, K. T., and Levine, R., 1956, *J. Am. chem. Soc.*, **78,** 2268.
[15] Collman, J. P., and Hoffman, N. W., 1973, *J. Am. chem. Soc.*, **95,** 2689.
[16] Even less anticipated is our observation that the methacrylate of F7(CHOH)H8 is also liquid-crystalline and forms what appears by optical microscopy to be a smectic B phase at low temperatures. Details concerning the methacrylates of F7(CHOH)H8 and F9(CHOH)H10 and their polymers will be presented in a future publication.
[17] Harris, R. K., and Mann, B. E., 1978, *NMR and the Periodic Table* (Academic Press), p. 98.
[18] Dungan, C. H., and van Wazer, J. R., 1970, *Compilation of Reported* ^{19}*F NMR Chemical Shifts* (Wiley-Interscience).
[19] Vilalta, P. M., Hammond, G. S., and Weiss, R. G., 1991, *Photochem. Photobiol.*, **54,** 563.
[20] Sackmann, H., and Demus, D., 1973, *Molec. Crystals liq. Crystals*, **21,** 239.
[21] Vinogradov, S. N., and Linnell, R. H., 1971, *Hydrogen Bonding* (Van Nostrand Reinhold Company).
[22] Demus, D., and Richter, L., 1978, *Textures of Liquid Crystals* (Deutscher Verlag für Grundstoffindustrie).
[23] Gray, G. W., and Goodby, J. W. G., 1984, *Smectic Liquid Crystals* (Leonard Hill).
[24] Bondi, A., 1964, *J. phys. Chem.*, **68,** 441. The van der Waals radii were taken to be 1·50 (doubly bonded oxygen atom), 1·52 (singly bonded oxygen atom), 1·70 (carbon atom), 1·47 (fluorine atom), and 1·20 (hydrogen atom), and 1·96 Å (iodine atom).
[25] Weast, R. C. (editor), 1979, *Handbook of Chemistry and Physics*, 59th edition (CRC Press), F-215 ff. Covalent bond lengths were 1·10 (C–H), 1·43 (C–O), 1·23 (C=O), 0·956 (O–H), 1·36 (C–F), 1·54 (C–C), and 2·14 Å (C–I).
[26] Ferguson, L. N., 1975, *Organic Molecular Structure* (Willard Grant Press), p. 57.